

IAC-18-C1.8.9

LOW-THRUST TRAJECTORY DESIGN VIA DIRECT TRANSCRIPTION LEVERAGING STRUCTURES FROM THE LOW-THRUST RESTRICTED PROBLEM

Robert Pritchett

Purdue University, USA, pritcher@purdue.edu

Andrew D. Cox

Purdue University, USA, cox50@purdue.edu

Kathleen C. Howell

Purdue University, USA, howell@purdue.edu

David C. Folta

NASA Goddard Space Flight Center, USA, david.c.folta@nasa.gov

Daniel Grebow

Jet Propulsion Laboratory - California Institute of Technology, USA, daniel.grebow@jpl.nasa.gov

A primary challenge of low-thrust mission design is the development of an initial guess for the state and control history of a trajectory. To address this challenge, one technique assembles dynamical structures, such as periodic orbits and their associated manifolds, into discontinuous chains that are corrected to locally optimal transfer solutions via direct transcription. In this investigation, dynamical structures that leverage a low-thrust force in a multi-body regime are incorporated into the orbit chain to expand the options available for construction of an initial guess and to guide the direct transcription algorithm toward different categories of locally optimal solutions. The properties and structures of the low-thrust model that facilitate orbit chain construction are demonstrated in representative transfer scenarios. Direct transcription is applied to converge upon locally optimal transfer trajectories in both simplified and ephemeris models. Results indicate that low-thrust dynamical structures offer a promising catalog of options in an orbit chain approach for designing optimal low-thrust trajectories.

I. INTRODUCTION

The efficiency of low-thrust propulsion has enabled a variety of ambitious missions in recent decades^{1,2} and encouraged the proposal of many new concepts to leverage this technology for exploration of the solar system.³⁻⁵ The growing use of low-thrust propulsion necessitates the improvement of strategies to design and navigate low-thrust trajectories. One of the primary challenges of low-thrust mission design is the development of an appropriate initial guess for the combined state and control history along a trajectory. While many strategies exist to leverage dynamical structures in two- and three-body models for ballistic trajectory design, fewer methods are available to supply an initial control history. This investigation seeks to leverage structures from a combined low-thrust, multi-body model to facilitate such preliminary planning. By incorporating these structures in a direct transcription scheme, low-thrust transfers between various regions of the three-body environ-

ment are designed and validated.

One technique for addressing the challenge of low-thrust trajectory design assembles dynamical structures, such as periodic orbits and their associated manifolds, into discontinuous chains that are corrected to locally optimal transfer solutions via direct transcription.^{6,7} Typically, the links employed in this orbit chain approach are ballistic trajectories, and thrust arcs are added during the corrections process to facilitate convergence and remove discontinuities between links. However, employing only natural arcs in an initial guess may obscure families of mass or time optimal trajectories that possess different geometries and control histories. One strategy that may mitigate this possibility is the incorporation of dynamical structures that leverage a low-thrust force in an orbit chain. These additional structures expand the options available for the construction of an initial guess and guide the direct transcription algorithm toward alternative sets of locally optimal solutions. In this investigation, a low-thrust (LT) force

is added to the equations that define the circular restricted three-body problem (CR3BP) to construct a combined model, the CR3BP-LT. Techniques from dynamical systems theory are applied to gain insight into the combined dynamics and to generate a variety of useful structures. Representative transfer scenarios demonstrate the construction of orbit chains that supply new geometries and reduce state discontinuities between links by leveraging these structures. Furthermore, insights from the CR3BP-LT model inform the selection of arcs in an orbit chain and guide the formulation of a feasible control history. Following orbit chain assembly, direct transcription is applied to converge upon locally optimal transfer trajectories in the CR3BP. Finally, the optimal paths are transitioned to a high-fidelity model for validation. Results indicate that an orbit chain containing low-thrust dynamical structures delivers optimal low-thrust trajectories and renders results as successfully as a chain that contains only ballistic structures. Moreover, a method employing low-thrust dynamical structures is adaptable, because these structures can be generated for a wide variety of system and spacecraft models as well as many different transfer scenarios. The application of low-thrust structures is particularly useful for transfer design between stable or nearly stable orbits that do not possess natural manifolds to facilitate flow to and from the orbits. Overall, low-thrust dynamical structures offer a promising catalog of options in support of an orbit chain approach to designing optimal low-thrust trajectories.

II. BACKGROUND

Multiple authors have explored techniques for low-thrust trajectory design similar to the chaining approach leveraged in this investigation.^{6,7} For example, Howell, Barden, and Lo apply this strategy within the context of the CR3BP to link invariant manifolds between periodic orbits for eventual application in support of the GENESIS mission.⁸ This application of dynamical systems theory to trajectory design has been further developed by a variety of researchers who utilize invariant manifolds to form *dynamical chains* that reveal natural flow in a wide range of three-body systems, and facilitate transfer design.^{9–13} Parker and others similarly employ a chaining approach to link periodic orbits and their manifolds to form complex new periodic orbits.^{14,15} Recently, Restrepo and Russell detailed an approach they titled “Patched Periodic Orbits” that leverages an extensive database of periodic orbits¹⁶ to quickly

design low-energy transfers throughout the CR3BP by linking successive periodic orbits.^{17,18} While the work of these authors includes many different applications, each employs a chaining strategy to link dynamical structures as a straightforward and practical approach to trajectory design. The present investigation builds upon these developments and seeks to further alleviate the challenge of low-thrust trajectory design in the CR3BP by assembling chains of ballistic and low-thrust dynamical structures.

Given the frequently large discontinuities between links in an orbit chain, collocation offers advantageous convergence properties for corrections. Collocation is an implicit numerical integration method that approximates the solution to a set of ordinary differential equations using polynomials. This approach is particularly robust compared to other methods because collocation algorithms are often able to converge upon a solution given a poor initial guess even when other techniques fail and can potentially be guided into a convergence basin of choice by exploiting specific structures. When paired with an optimization algorithm, the resulting scheme is denoted *direct transcription*.¹⁹ In this scheme, collocation is employed to discretize a continuous optimal control problem into a nonlinear programming problem (NLP) that is then solved via a direct optimization approach. Grebow and Pavlak²⁰ offer an overview of the history of collocation and direct transcription methods, and these techniques are discussed more generally within several excellent survey papers on the topic of trajectory optimization.^{21–23} Many possible implementations of a direct transcription scheme are available; this investigation generally follows the collocation and mesh refinement framework defined by Grebow and Pavlak,²⁰ and is consistent with previous work.^{6,7} Direct transcription has been leveraged previously to explore solutions to low-thrust trajectory design problems in the Earth-Moon CR3BP.^{24–27} This earlier work demonstrates that direct transcription successfully delivers a solution for a wide range of initial guess and path constraint scenarios. Overall, the robustness and adaptability of direct transcription offers a powerful strategy for computing low-thrust solutions.

Although direct transcription possesses a wide basin of convergence, the generation of initial guesses for low-thrust paths through multi-body regimes remains challenging and can influence the results obtained from collocation. While there are many strategies for designing thrust vector histories in the two-body problem^{28,29}, fewer methods incorporate multi-

body dynamics. Studies of solar sail dynamics in the Earth-Sun and Earth-Moon three-body systems supply some guidance on the selection of sail parameters to achieve stable orbits around artificial equilibria³⁰, or paths between sequences of artificial equilibria.³¹ Subsequent studies of the combined CR3BP-solar sail dynamics problem reveal a rich variety of dynamical structures, including invariant manifolds, periodic orbits, and quasi-periodic orbits.^{32,33} Similar structures exist in a more general low-thrust, multi-body model, the CR3BP-LT, and are leveraged to identify initial guesses for a low-thrust control history.^{34,35} Dynamical structures and insights from the low-thrust CR3BP (CR3BP-LT) are employed in this investigation to construct initial designs that incorporate low-thrust.

III. DYNAMICAL MODEL DEVELOPMENT

The first step in constructing and leveraging dynamical structures for inclusion in a low-thrust trajectory design is the development of the dynamical model. An energy-based approach is first employed to derive the governing equations in the CR3BP and obtain an expression for the natural Hamiltonian. By augmenting the CR3BP equations of motion (EOMs) with a low-thrust term, the CR3BP-LT is constructed and the associated low-thrust Hamiltonian is defined. This low-thrust Hamiltonian serves as an integral of the motion when the low-thrust acceleration vector is fixed in the rotating frame, and, thus, may be leveraged to characterize motion in the CR3BP-LT. Finally, transfers constructed within the CR3BP are transitioned to an N -body ephemeris model for validation.

III.i Circular Restricted Three-Body Problem

The CR3BP describes the motion of a relatively small body, such as a spacecraft, in the presence of two larger gravitational point masses (P_1 and P_2) with paths that evolve along circular orbits about their mutual barycenter (B). To simplify the governing equations and enable straightforward visualization of periodic solutions, the motion of the spacecraft is described in a right-handed frame (\hat{x} , \hat{y} , \hat{z}) that rotates with the two primaries, as seen in Figure 1, where \hat{x} , \hat{y} , and \hat{z} are vectors of unit length (denoted by the caret above the symbol). The system is parameterized by the mass ratio, $\mu = M_2/(M_1 + M_2)$, where M_1 and M_2 are the masses of the primaries and $M_1 \geq M_2$. To facilitate numerical integration, the dimensional values are nondimensionalized by characteristic quantities such that the distance between

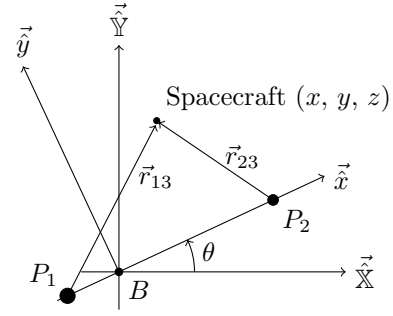


Fig. 1: CR3BP system configuration; two point masses, P_1 and P_2 , proceed on circular orbits about their mutual barycenter, B . The behavior of a third, relatively massless particle is described via the rotating coordinate frame, $(\hat{x}, \hat{y}, \hat{z})$

P_1 and P_2 is unity, the mean motion of the two primaries is unity, and the masses of each body range from zero to one.³⁶

The equations of motion governing the CR3BP are derived via a Hamiltonian energy approach. Let the kinetic (T) and potential (V) energies corresponding to the CR3BP system be defined by

$$T = \frac{1}{2} \left[(\dot{x} - \dot{y})^2 + (\dot{y} + \dot{x})^2 + \dot{z}^2 \right], \quad [1]$$

$$V = \frac{-(1 - \mu)}{r_{13}} - \frac{\mu}{r_{23}}, \quad [2]$$

where \dot{x} , \dot{y} , and \dot{z} are the derivatives of the position states with respect to nondimensional time as observed in the rotating frame, and r_{13} and r_{23} are the distances between the spacecraft (P_3) and the first and second primaries, respectively:

$$r_{13} = \sqrt{(x + \mu)^2 + y^2 + z^2},$$

$$r_{23} = \sqrt{(x - 1 + \mu)^2 + y^2 + z^2}.$$

Next, form the Hamiltonian,

$$H_{nat} = \frac{1}{2}v^2 - \frac{1}{2}(x^2 + y^2) - \frac{1 - \mu}{r_{13}} - \frac{\mu}{r_{23}}, \quad [3]$$

where $v^2 = \dot{x}^2 + \dot{y}^2 + \dot{z}^2$ is the spacecraft velocity magnitude in the rotating frame. By applying Hamilton's canonical equations of motion, a set of differential equations that govern the motion of P_3 emerges,

$$\ddot{x} = 2\dot{y} + \Omega_x, \quad [4]$$

$$\ddot{y} = -2\dot{x} + \Omega_y, \quad [5]$$

$$\ddot{z} = \Omega_z, \quad [6]$$

where Ω is the CR3BP *pseudo-potential* function,

$$\Omega = \frac{1}{2}(x^2 + y^2) + \frac{1 - \mu}{r_{13}} + \frac{\mu}{r_{23}}, \quad [7]$$

and Ω_x , Ω_y , and Ω_z represent the partial derivatives of Ω with respect to the subscripted variables x , y , and z . Because the CR3BP is autonomous and conservative, H_{nat} is constant and proportional to the Jacobi integral, i.e., the *Jacobi constant*. The Jacobi constant, $C = -2H_{nat}$, is commonly used as a measure of the energy associated with arcs in the CR3BP.

III.ii CR3BP Incorporating Low-Thrust

To incorporate low-thrust into the CR3BP multi-body model, the low-thrust acceleration vector is first defined. This vector,

$$\vec{a}_{lt} = \frac{f}{m} \hat{u}, \quad [8]$$

is oriented relative to the rotating frame via the unit vector \hat{u} and scaled by the nondimensional thrust magnitude, f , and nondimensional spacecraft mass, $m = M_3/M_{3,0}$, where M_3 is the instantaneous spacecraft mass and $M_{3,0}$ is the initial (wet) spacecraft mass. A nondimensional thrust magnitude of $f \approx 10^{-2}$ in the Earth-Moon and Sun-Earth CR3BP-LT systems is consistent with current spacecraft capabilities, such as Deep Space 1, Dawn, or Hayabusa.^{34,35} Accordingly, a low-thrust acceleration magnitude of $a_{lt} = f/m = 7e-2$ is frequently employed in this analysis to represent a reasonable low-thrust capability, approximately 0.19 mm/s^2 in the Earth-Moon system.

To apply an energy-based derivation of the CR3BP-LT EOMs similar to the derivation leveraged for the CR3BP, the CR3BP dynamics are augmented with a low-thrust acceleration term. While the spacecraft kinetic energy expression in Equation [1] remains unchanged, the potential energy expression incorporates a low-thrust acceleration term, i.e.,

$$V_{lt} = \frac{-(1 - \mu)}{r_{13}} - \frac{\mu}{r_{23}} - \vec{r} \cdot \vec{a}_{lt}, \quad [9]$$

where $\vec{r} = \{x \ y \ z\}^T$. This additional term propagates through the derivation to yield the low-thrust Hamiltonian,

$$H_{lt} = \frac{1}{2}v^2 - \frac{1}{2}(x^2 + y^2) - \frac{1 - \mu}{r_{13}} - \frac{\mu}{r_{23}} - \vec{r} \cdot \vec{a}_{lt}, \quad [10]$$

which may also be written in terms of the natural Hamiltonian, i.e.,

$$H_{lt} = H_{nat} - \vec{r} \cdot \vec{a}_{lt}. \quad [11]$$

Due to the time-varying nature of the spacecraft mass, the governing equations are not available directly from Hamilton's canonical equations. However, Newton's law is applied to yield the EOMs,

$$\ddot{x} = 2\dot{y} + \Omega_x + a_{lt}u_x, \quad [12]$$

$$\ddot{y} = -2\dot{x} + \Omega_y + a_{lt}u_y, \quad [13]$$

$$\ddot{z} = \Omega_z + a_{lt}u_z, \quad [14]$$

$$\dot{m} = \frac{-fl_*}{I_{sp}g_0t_*}, \quad [15]$$

where a_{lt} is the low-thrust acceleration vector magnitude, u_x is the \hat{x} -component of \hat{u} , u_y is the \hat{y} -component, and u_z is the \hat{z} -component. Additionally, I_{sp} is the specific impulse associated with the propulsion system, and $g_0 = 9.80665 \times 10^{-3} \text{ km/s}^2$. These equations are consistent with those that govern the natural CR3BP and are augmented with the low-thrust acceleration terms.

To facilitate analyses in the CR3BP-LT, simplifications are applied to reduce the number of dimensions. The natural problem, which is conservative, admits an integral of the motion (the Hamiltonian, H_{nat}), reducing the natural problem dimension by one. Due to the non-autonomous nature of the CR3BP-LT, the low-thrust Hamiltonian is not constant in general and, thus, does not offer a similar dimension reduction. However, when the magnitude and orientation of the low-thrust acceleration vector are fixed in the rotating frame, H_{lt} is constant, yielding a conservative, Hamiltonian system. A constant \vec{a}_{lt} vector is a reasonable assumption in CR3BP-LT systems with sufficiently small l_*/t_* ratios and sufficiently large μ values, such as the Earth-Moon system employed in this investigation.³⁵ Accordingly, the variable acceleration quantity f/m is replaced by the constant value a_{lt} , removing the need for the mass time-derivative in Equation [15]. These simplifications – a constant low-thrust Hamiltonian and a constant acceleration magnitude – effectively reduce the problem dimension to simplify analyses.

By leveraging the constant low-thrust acceleration vector simplification, additional insights are available to guide low-thrust trajectory design. While the natural Hamiltonian is not generally constant in the CR3BP-LT, H_{nat} evolves independently of the spacecraft path when \vec{a}_{lt} is fixed in the rotating frame.³⁵ Finally, to further reduce the system complexity, only planar motion is considered. That is, $z(\tau) = \dot{z}(\tau) = 0$ for all τ , and the planar low-thrust pointing vector, \hat{u} , is described by the vector

$$\hat{u} = \{\cos \alpha \quad \sin \alpha \quad 0\}^T. \quad [16]$$

These simplifications facilitate the study of dynamical structures in the CR3BP-LT while also supplying insights that are useful for spatial (3D) trajectory design.

III.iii *N*-Body Ephemeris Model

Transfers constructed in a simplified three-body dynamical model must be validated in an N -body ephemeris based model before they can be applied to realistic spaceflight scenarios. The establishment of an ephemeris model begins with the definition of an inertial reference frame. By convention, the origin of this frame is located at the center of one of the gravitational bodies included in the model with mass denoted m_q . The motion of the particle of interest, with mass m_i , is influenced by the central body and expressed within this inertial reference frame. Other gravitational bodies, m_j , included in the ephemeris model exert additional perturbing influences on the particle of interest. All bodies are assumed to be centrobatic point masses, thus, the equations of motion for the particle of interest are,

$$\ddot{\vec{p}}_{qi} = -G \frac{m_i + m_q}{p_{qi}^3} \vec{p}_{qi} + G \sum_{\substack{j=1 \\ j \neq i, q}} m_j \left(\frac{\vec{p}_{ij}}{p_{ij}^3} - \frac{\vec{p}_{qj}}{p_{qj}^3} \right) \quad [17]$$

where G is the universal gravitational constant, \vec{p}_{qi} is the position vector from the central body to the particle of interest, and p_{qi} is the norm of this vector. Likewise, \vec{p}_{ij} and \vec{p}_{qj} are position vectors to the perturbing bodies from the particle of interest and the central body, respectively. In this investigation the Earth or Moon are employed as the central body, while the Sun and Jupiter are included as additional perturbing bodies. The locations of these bodies are obtained from the Jet Propulsion Laboratory's Navigation and Ancillary Information Facility (NAIF) SPICE ephemeris data, specifically the DE421 ephemerides.³⁷ The particle of interest in this application is assumed to be a low-thrust spacecraft with an infinitesimally small mass compared to the masses of the other bodies. Finally, the states of all bodies are expressed in the J2000 inertial frame and the initial epoch is noon UTC on January 1st, 2000. Together, these parameters define the ephemeris model employed to validate trajectories.

IV. DYNAMICAL STRUCTURES

Initial low-thrust trajectory designs may exploit a variety of dynamical structures, including both ballistic CR3BP arcs and thrust-enabled motion from

the CR3BP-LT. A preliminary understanding of the structures available for any model results from an analysis of the local linear dynamics near the equilibrium solutions. From this basic analysis, numerical algorithms globalize the local dynamics to yield families of structures, such as periodic and quasi-periodic orbits, that may be employed as destination orbits or might deliver intermediate arcs. Finally, dynamical systems techniques are applied to periodic orbits to construct manifolds that offer low-cost transfers into and out of the originating structure. As manifolds frequently exist for both ballistic and low-thrust periodic solutions, they are a valuable component of orbit chains for low-thrust trajectory design.

IV.i Equilibrium Solutions

The planar dynamics in the CR3BP yield equilibrium solutions that supply an initial characterization of the local and global dynamics that may be utilized for path planning. Given the nonlinear dynamics, linear variational behavior relative to the equilibria is reflected via local stable, unstable, and center manifolds. Global invariant manifolds are constructed by transitioning the linear results to the nonlinear model, where they are leveraged for trajectory design.³⁶ The CR3BP admits five equilibrium solutions, the well known *Lagrange points*. Three *collinear* points, i.e., L_1 , L_2 , and L_3 , are located on the rotating x -axis and are characterized by a saddle and a center subspace. Accordingly, stable and unstable manifolds supply transit motion to and from these equilibria (the saddle mode), and oscillatory solutions exist near the fixed point (the center mode). The triangular points, i.e., L_4 and L_5 , do not possess a saddle mode and are characterized by a four-dimensional center subspace in the Earth-Moon CR3BP. Subsequently, no manifolds describe flow to or from these fixed points. Periodic and quasi-periodic structures are initialized from linear approximations supplied by the center subspace associated with each equilibrium point, yielding families of structures such as the well-known planar Lyapunov orbits near L_1 , L_2 , and L_3 and the short period orbits (SPOs) near L_4 and L_5 .

Similar to the CR3BP, the planar CR3BP-LT admits equilibrium solutions that supply useful flow characterizations. However, the locations, local linear dynamics, and number of equilibrium points vary with the thrust magnitude and its orientation.^{34,35} Subsequently, manipulations of the low-thrust acceleration vector directly influence the existence and characteristics of nearby dynamical structures. When a_{lt} is small, the CR3BP-LT equilibria are located near

the natural equilibrium points and are characterized by similar linear modes. However, as a_{lt} increases, the low-thrust equilibria move further from the natural fixed points and the associated stability characteristics change, both qualitatively (e.g., saddle, center) and quantitatively (e.g., time constant, frequency). These variations between the natural and low-thrust equilibrium solutions supply novel flow patterns that are employed to inform initial guesses for low-thrust transfers.

IV.ii Periodic Solutions

Periodic solutions in the CR3BP are important components of many trajectory design applications as they supply bounded, repeated motion in space while accounting for third-body effects, a level of fidelity not available in the conic model. Additionally, periodic motion from the CR3BP is transitioned to ephemeris models via corrections algorithms.³⁸ Many families of periodic solutions originate from the equilibrium solutions; very near the fixed point, the nonlinear periodic motion is well approximated by the local linear dynamics of the center subspace. Continuation methods are then employed to compute additional solutions that are affected more strongly by the nonlinearities of the global dynamics. These *families* of dynamical structures are parameterized by a single quantity, such as the Jacobi constant (or, equivalently, H_{nat}), orbital period, or a nonphysical parameter. Accordingly, structures are selected from a family based on the set of characteristics required for a mission application.

Periodic solutions are also available in the CR3BP-LT, with many families of these structures also originating near the low-thrust equilibrium solutions that possess a center subspace. As the equilibria locations and stability properties vary from the natural CR3BP conditions as a function of the low-thrust magnitude, a_{lt} , and orientation angle, α , families of solutions are available in the CR3BP-LT that do not exist in the natural problem, such as those plotted in Figure 2. Similar to families of orbits in the CR3BP, low-thrust periodic orbit families are parameterized by a single value such as H_{lt} , orbital period, α , or a_{lt} . For example, the family of orbits in Figure 2 evolves with α ; each family member is characterized by the same $H_{lt} = -1.453$ value. Each orbit within this family is also a member of a family that evolves through a range of H_{lt} values with a fixed α value. Thus, given the increased dimension of the CR3BP-LT, families may be continued along a greater number of dimensions, yielding a larger set of solutions for use in an

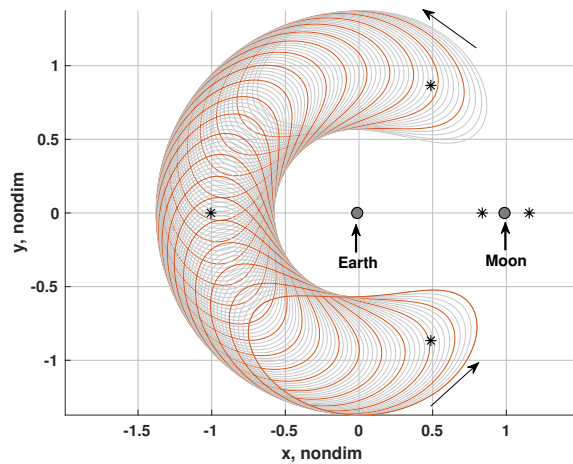


Fig. 2: Family of periodic orbits in the Earth-Moon CR3BP-LT for $a_{lt} = 7e-2$ and $H_{lt} = -1.453$; each family member corresponds to a different orientation angle, α

initial trajectory design. Furthermore, as α and a_{lt} are both available as continuation parameters, links between the spacecraft thrust history and the trajectory geometry are available from these solutions.

IV.iii Manifolds

Invariant manifolds associated with periodic orbits describe flow through the CR3BP.³⁹ Similar to the equilibrium solutions, linear dynamics derived from the stroboscopic representation of a periodic orbit may be characterized as saddle modes with stable and unstable manifolds, or as center modes that indicate additional oscillatory motion, i.e., quasi-periodic solutions. As the stable and unstable manifolds asymptotically approach the periodic solution in reverse and forward time, respectively, they are frequently exploited as pathways between periodic structures, for example in the design approach for missions like GENESIS.⁴⁰ The manifolds associated with a periodic orbit, by necessity, are characterized by the same properties as the originating structure. To clarify, manifolds of a CR3BP orbit possess the same H_{nat} value as the orbit, and manifolds emerging from a CR3BP-LT orbit are characterized by the same H_{lt} , α , and a_{lt} values as the low-thrust periodic structure. Accordingly, the manifolds associated with low-thrust periodic orbits (LTPOs), such as those depicted in Figure 3, supply additional links between geometric paths through space and specific sets of control parameters (α and a_{lt}), facilitating the construction of an initial transfer design with a priori

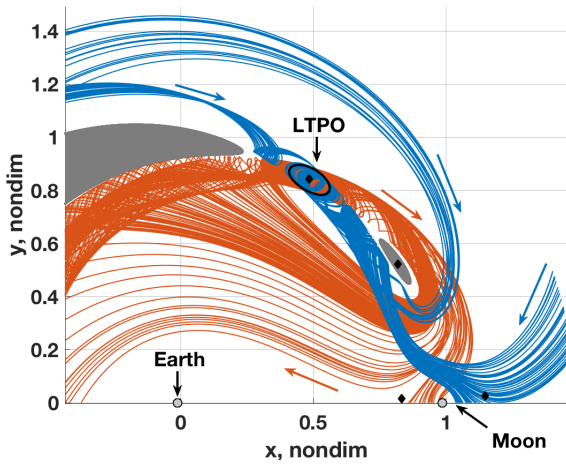


Fig. 3: Stable (blue) and unstable (orange) manifolds associated with a low-thrust periodic orbit (LTPO) in the Earth-Moon CR3BP-LT for $a_{lt} = 7e-2$, $\alpha = 60^\circ$, and $H_{lt} = -1.562$. Forbidden regions corresponding to this H_{lt} value (gray regions) bound the low-thrust motion; low-thrust equilibria are plotted as black diamonds

knowledge of the thrust profile.

V. RESULTS

Dynamical structures from the CR3BP and CR3BP-LT are combined in chains to design transfers for two different applications. In each application, a chain of only natural structures and a chain with structures from both models are utilized as initial designs for the direct transcription algorithm. The objective function for this formulation is maximum final mass, and the total change in mass along a trajectory, Δm , is one of the parameters used to compare results. Other characteristics such as geometry and thrust profile are also employed to draw comparisons and explore the impact of the low-thrust structures on the optimal trajectory delivered by direct transcription. Results demonstrate that when the geometries of two orbit chains are similar (regardless of the model that delivers the component structures), comparable optimal solutions are computed, and vice versa. In this investigation, solutions with broadly similar characteristics are described as existing in the same optimal “basins”. This application of the term “basin” is looser than the mathematical definition of the word; however, within this context, it is a useful term for grouping the types of optimal solutions that result from a variety of initial trajectory designs. The versatility of the orbit chain framework

is extended when low-thrust structures are included in an initial guess, because such structures offer novel geometries for some applications. Thus, the optimal solution may be intentionally biased to certain basins by selecting low-thrust arcs with desirable properties.

V.i Transfer Application 1: L_4 SPO to L_3 Lyapunov

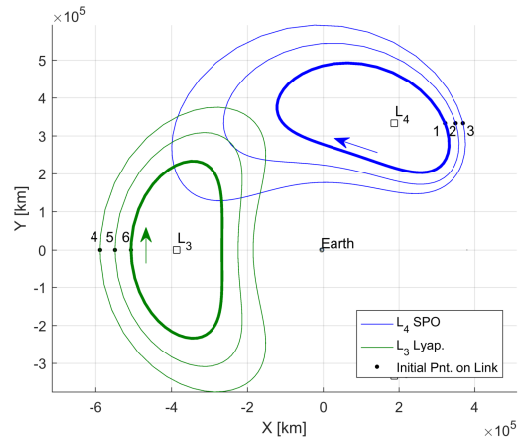
Families of low-thrust periodic orbits offer new geometries and energy profiles that may be employed to aid the process of low-thrust trajectory design. Moreover, in contrast to natural dynamical structures, low-thrust dynamical pathways include prescribed control histories, and these may offer an improved initial guess for the control profile necessary to achieve a feasible transfer. In this sample application, members of a family of low-thrust periodic orbits are utilized in an orbit chain technique to comprise an initial guess for a low-thrust transfer from an L_4 short period orbit (SPO) to an L_3 Lyapunov orbit, both characterized by the natural Hamiltonian value $H_{nat} = -1.453$. The same general transfer concept is also developed using an orbit chain consisting of only natural dynamical structures from the CR3BP as an initial guess. The low-thrust periodic orbits utilized in the former case prescribe a control history; however, in both initial designs, when ballistic arcs are employed the control history is defined such that the thrust vector has zero magnitude and is aligned with the velocity vector. Contrasting the two different initial guesses demonstrates the use of the low-thrust dynamical structures in the transfer design process and the resulting final trajectory.

An orbit chain consisting of only natural dynamical structures from the CR3BP is assembled as an initial guess for the planar transfer between the aforementioned L_4 SPO and L_3 Lyapunov orbits. In addition to the initial and final orbits, several other members of the L_4 SPO and L_3 Lyapunov orbit families are included as intermediate links in the orbit chain, as seen in Figure 4(a). These additional links are added to reduce the discontinuities in position and velocity between subsequent members of the orbit chain. The inclusion of these supplementary links necessitates a change in energy, demonstrated in Figure 4(b) with a plot of H_{lt} as a function of orbital period for the L_4 SPO and L_3 Lyapunov families. Note that the low-thrust Hamiltonian is equivalent to the natural Hamiltonian, H , for natural arcs as the low-thrust acceleration magnitude, a_{lt} , is zero, negating the extra terms in Equation [10]; H_{lt} is used for consistency when both low-thrust and natural arcs are included in the chain. Figure 4(b) illustrates that the addi-

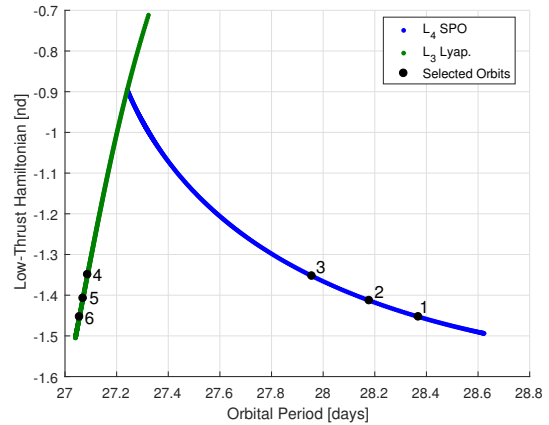
tional members of the L_4 SPO family increase the value of H_{lt} with increasing distance from the originating SPO, while the extra L_3 Lyapunov orbits decrease this value again with decreasing distance to the destination Lyapunov. Furthermore, the third and fourth orbit chain links are selected to possess the same H_{lt} value, to aid in reducing the energy change required to transition between periodic orbit families. More intermediate links, including additional orbits from either the L_4 SPO or L_3 Lyapunov orbit families, could be added to further reduce discontinuities; however, the inclusion of additional orbits yields an increased time-of-flight and a larger number of design variables in the optimization problem. Rather, it is advantageous to include alternative dynamical structures that offer paths that span the region of interest and reduce the discontinuities observed within the initial guess.

As an alternative to a chain of purely ballistic arcs, an orbit chain that leverages a unique family of L_4 LTPOs is assembled. The family of L_4 LTPOs leveraged in this transfer is defined by $H_{lt} = -1.453$ and is displayed in Figure 2. This family of LTPOs is selected because its members neatly span the space between the natural departure and destination orbits. Therefore, four orbits from this family are employed in an orbit chain that also includes the natural initial and final orbits. Figure 5(a) illustrates the consecutive links of this orbit chain and their overlap at multiple points in position space; the intermediate links gradually transition the direction of velocity from the departure to the destination orbits. These LTPOs offer reduced position and velocity discontinuities between orbit chain links and they maintain a value of H_{lt} consistent with the initial and final orbits, as apparent in Figure 5(b). The H_{lt} value along each low-thrust periodic orbit is consistent with the initial and final natural orbits. Additionally, the size in configuration space and the velocity along each of the links are similar. These notable observations may facilitate convergence and offer an alternative geometry compared to the stack of natural orbits in Figure 4(a). A chain constructed from arcs with similar energy values may yield a transfer with lower propellant costs, but other variables (orbit orientation, velocity direction) strongly influence convergence and the resulting optimal solution.

The two different orbit chains are then used as initial guesses for the direct transcription algorithm and the results are compared. Observe that the mass optimal transfers computed from each guess are quite similar, as plotted in Figure 6. Both transfers ex-



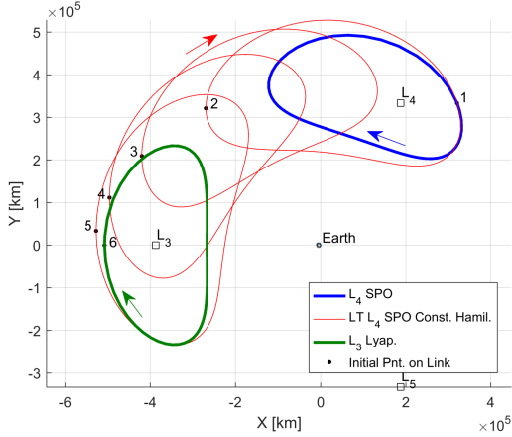
(a) Selected members of the L_4 SPO and L_3 Lyapunov orbit families including the initial and final orbits (bolded).



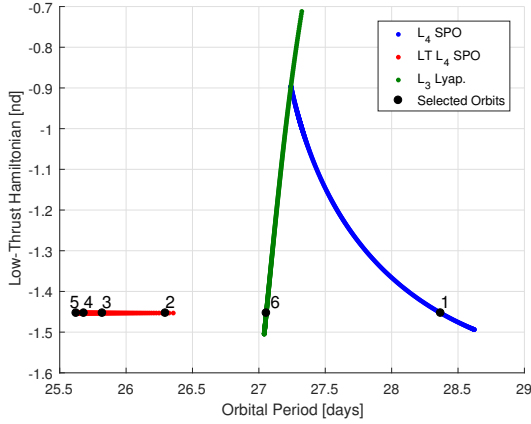
(b) Plot of H_{lt} as a function of orbital period for the orbit families used to construct initial guess.

Fig. 4: Natural periodic orbits are employed to compose an initial guess for a transfer from an L_4 SPO to an L_3 Lyapunov orbit. Geometry and energy characteristics are examined to select the components or links of the initial guess.

hibit nearly identical geometries with thrust segments in very similar locations. Both employ brief thrust segments for departure and insertion as well as two longer thrust segments during intermediate arcs. The small differences between the two solutions become more apparent when their energy profiles, plotted in Figure 7, are examined. These profiles display H_{lt} as a function of time-of-flight for both transfers. While these profiles are similar, it is evident that the transfer generated with the orbit chain comprised of only natural dynamical structures deviates more fre-



(a) Selected members of a low-thrust L_4 SPO family at $H_{lt} = -1.453$ along with the departure L_4 SPO and arrival L_3 Lyapunov (bolded).



(b) Plot of H_{lt} as a function of orbital period for the orbit families employed to construct initial guess.

Fig. 5: Low-thrust periodic orbits are employed to compose an initial guess for a transfer from an L_4 SPO to an L_3 Lyapunov orbit. Geometry and energy characteristics are examined to select the components of the initial guess.

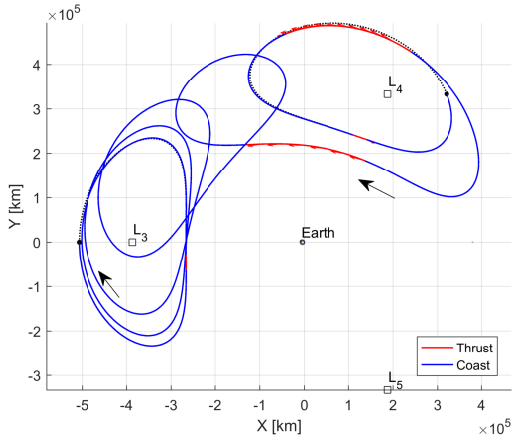
quently and farther from the H_{lt} value corresponding to the initial and final orbits. Prior to the first long duration burn, the energy profile in Figure 7(a) deviates from the initial value of H_{lt} more significantly than the profile in Figure 7(b) that corresponds to the solution initialized with low-thrust structures. Furthermore, the coast arc bounded by the two long-duration burns maintains a lower energy level for the transfer computed using only natural orbits; this difference corresponds to the slight variation in geometry for this arc between the two solutions (see Figure

Init. Guess	TOF [days]	Δm [kg]	ΔV [m/s]
Nat. Only	165.716	5.825	171.887
With LT	158.847	3.572	105.289

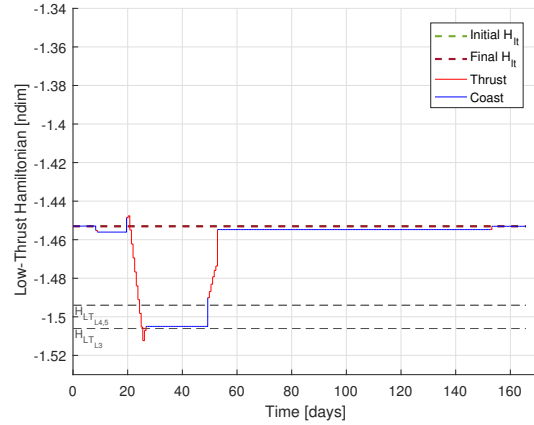
Table 1: Summary of key parameters for the low-thrust transfers computed in the Earth-Moon CR3BP for Application 1.

6). A transfer with minimal energy changes corresponds to the theoretical minimum-cost path, and this is likely the reason that the transfer generated using LTPOs requires a smaller Δm . The change in mass associated with both transfers computed in the CR3BP is summarized along with time-of-flight (TOF) and ΔV in Table 1. The reported ΔV values are computed from the classical rocket equation. This expression offers an approximation of the equivalent ΔV required for a low-thrust transfer.

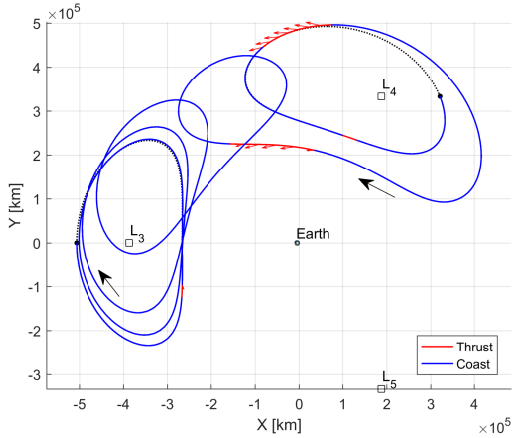
The transfer generated with the aid of low-thrust dynamical structures consumes over 2 kilograms less propellant, which translates to a ΔV savings of approximately 65 m/s. The nearly constant energy profile associated with the initial guess that includes low-thrust dynamical structures may guide the optimizer to a slightly more optimal solution. However, one sample application is not sufficient for any broad conclusions concerning the value of thrust enabled arcs in an initial guess. The similarities between the two solutions – despite the significantly different initial guesses – highlights the robustness of the direct transcription algorithm. Moreover, the result is consistent with previous efforts that demonstrate both the existence of multiple “basins”, i.e. many local minimums, in the solution space, and the impact of the links in an orbit chain that guides the optimal solution into one of these basins⁷. In this application, the orbit chains are sufficiently alike to guide the result to similar local optimal basins. However, chains incorporating other links are also successful. Although dynamical structures from the CR3BP-LT offer novel geometries, these structures may direct a path to a similar set of basins. Finally, to validate the transfers, both low-thrust transfers are transitioned to an N -body ephemeris model that includes the Earth, Moon, Sun, and Jupiter. This transition is successful, and the resulting transfers are displayed in Figure 8. Clearly, both transfers retain a geometry consistent with the transfers observed in the CR3BP.



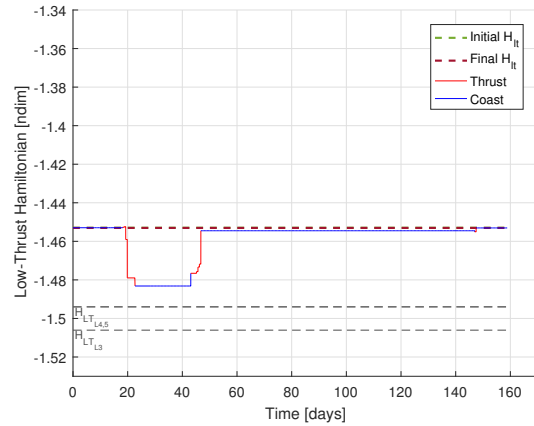
(a) Transfer from orbit chain initialized from only natural dynamical structures.



(a) Optimal transfer generated with natural dynamical structures.



(b) Transfer from orbit chain initialized with low-thrust periodic orbits.



(b) Optimal transfer generated with low-thrust dynamical structures.

Fig. 6: Direct transcription is employed to compute mass optimal low-thrust transfers using the orbit chain initial guesses.

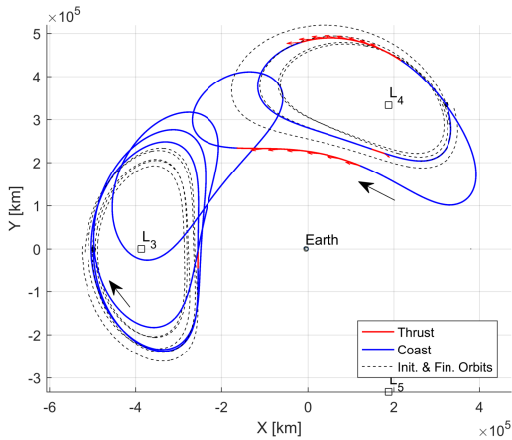
Fig. 7: The time history of the low-thrust Hamiltonian, H_{lt} , for each transfer offers insight on the energy evolution to achieve the transfer

V.ii Transfer Application 2: L_4 SPO to L_1 Lyapunov

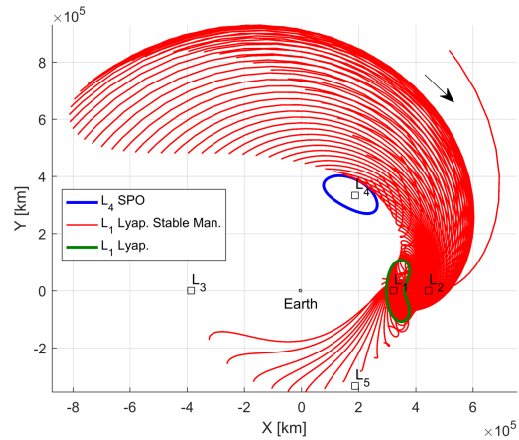
Low-thrust structures offer unique pathways that may differ significantly from the natural dynamics. For example, unstable LTPOs exist in the vicinity of stable natural periodic orbits. Accordingly, transfers to the natural periodic orbit can be facilitated by the LTPO stable and unstable manifolds that flow into and out of the region. To illustrate a transfer leveraging such structures, a trajectory is designed to deliver a spacecraft from an L_4 SPO with $H_{nat} = -1.487$ to an L_1 Lyapunov orbit with $H_{nat} = -1.503$. The orbit chain technique is employed to construct two different initial designs: (i) a chain of purely natural

orbits and their associated manifolds, and (ii) a chain that includes natural orbits as well as the manifold of a nearby L_4 LTPO. Once an initial guess is constructed, a direct transcription algorithm is employed to remove discontinuities in the solution, yielding a feasible design. Finally, the feasible solution is optimized to maximize the final spacecraft mass, and the solutions resulting from the two initial designs are compared.

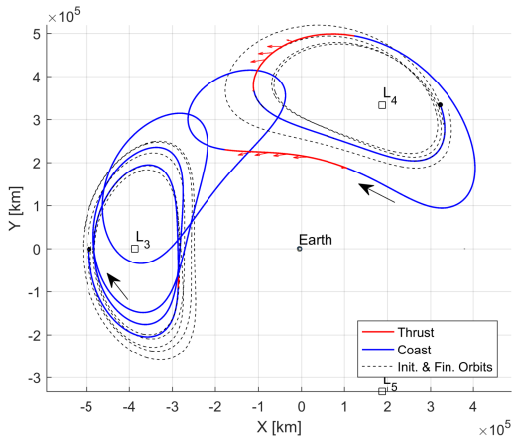
An orbit chain that delivers the spacecraft from the L_4 SPO to the L_1 Lyapunov is first constructed leveraging only dynamical structures from the natural CR3BP. Stable manifolds associated with the L_1 orbit, plotted in Figure 9(a), pass near the L_4 SPO



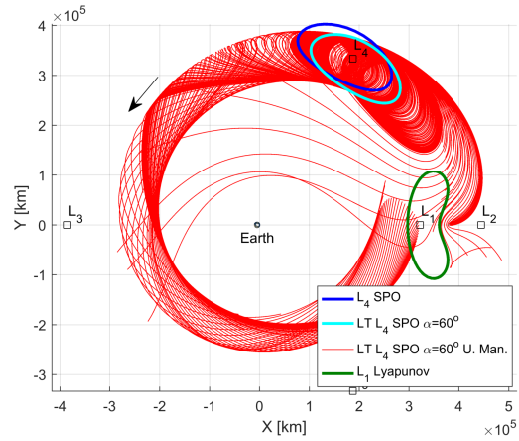
(a) Transfer generated with natural dynamical structures.



(a) Stable manifolds associated with an L_1 Lyapunov orbit possessing $H_{nat} = -1.503$ approach the L_4 SPO in reverse time.



(b) Transfer generated with low-thrust dynamical structures.



(b) Unstable manifolds for a low-thrust L_4 LTPO with $\alpha = 60^\circ$ and $H_{lt} = -1.553$ approach the lunar region from two directions.

Fig. 8: Direct transcription is employed to compute mass optimal low-thrust transfers in an N -Body ephemeris model using the CR3BP result as an initial guesses.

and offer a suitable geometry to facilitate the transfer. However, while these natural manifolds are located near the L_4 orbit in position space, a velocity discontinuity, i.e., an H_{nat} discontinuity, exists between the L_1 Lyapunov manifolds and the SPO. As the L_4 orbit is stable and does not possess manifolds, no additional natural structures to guide the flow are immediately apparent. To complete the transfer design, five revolutions along the initial L_4 orbit and a single revolution of the L_1 orbit are included. The five revolutions along the SPO are included so that the transfer time-of-flight (TOF) is similar to the design that utilizes a low-thrust manifold. In addition

Fig. 9: The invariant manifolds for a low-thrust L_4 LTPO offer different geometries than those of the destination L_1 Lyapunov manifold.

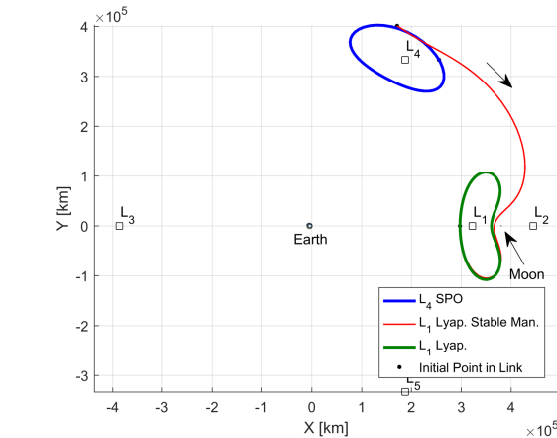
to adding transfer time, this stacking supplies ample time and space for the spacecraft to achieve the required energy change between the L_1 manifold and the L_4 SPO, facilitating convergence in the direct transcription algorithm.

The second transfer design offers an alternate geometry by leveraging low-thrust dynamical structures. While H_{nat} is constant along every natural structure, the addition of low-thrust implies an evolving H_{nat} value along low-thrust dynamical structures (H_{lt} , on the other hand, remains constant). Accordingly, both geometric and energetic paths may be in-

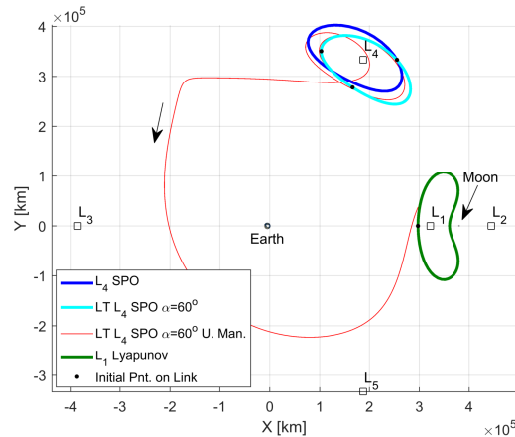
corporated with low-thrust structures. To accomplish the L_4 to L_1 transfer, an unstable LTPO with a similar geometry and energy value consistent with the natural L_4 SPO is identified to reduce position and velocity discontinuities between the two structures. The manifolds emerging from this low-thrust orbit, as plotted in Figure 9(b), offer an alternative set of pathways in position space to complete the transfer. To design the transfer, a single revolution of the natural L_4 SPO is included, followed by a manifold originating from the nearby L_4 LTPO and then two revolutions of the natural L_1 Lyapunov orbit.

In both scenarios, the manifold path best suited for a given orbit chain is selected by inspecting the total set of stable or unstable manifolds and identifying the manifold trajectory that demonstrates the closest intersection in position space with the adjacent orbit in the chain. Additionally, the direction and magnitude of the velocity vector at the end of the manifold trajectory is selected to be similar to that at the intersection point along the final orbit. The velocity states are directly employed as criteria for link selection in this case, rather than the analogous energy values examined previously. It is critically important to match velocity directions when linking the manifolds arcs to another dynamical structure. This shift in criteria is necessary because invariant manifolds at the same value of H_{nat} or H_{lt} can exhibit significantly different position and velocity profiles. Therefore, limiting velocity state differences when assembling an orbit chain can ensure the initial guess contains reasonably small discontinuities.

Following the prescribed manifold trajectory selection strategy, the initial designs for each transfer are constructed. The all-natural design, plotted in Figure 10(a), includes a direct path between the two periodic orbits via an L_1 stable manifold arc. The low-thrust design, plotted in Figure 10(b), leverages a low-thrust manifold trajectory that encircles the Earth before reaching the destination L_1 orbit. Both initial guesses are converged via direct transcription, first for feasibility, and then for mass-optimality. The final, optimized results, plotted in Figure 11, possess distinctly different geometries that are biased by the initial designs. The solution initialized with only natural structures, in Figure 11(a), approximately mirrors the initial geometry (Figure 10(a)) with a transfer approaching the L_1 Lyapunov from the right, consistent with the L_1 stable manifold. The solution leveraging low-thrust structures, plotted in Figure 11(b), also remains generally consistent with the initial geometry (Figure 10(b)), approaching the Lyapunov orbit from the left after encircling the Earth.



(a) Orbit chain with only natural dynamical structures

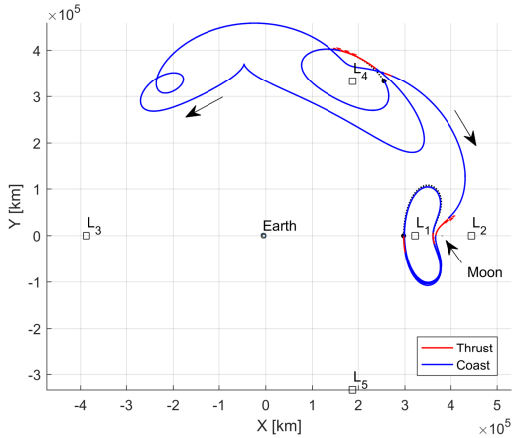


(b) Orbit chain with low-thrust dynamical structures

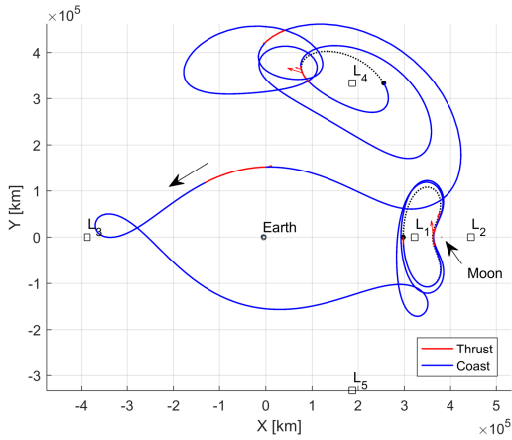
Fig. 10: The orbit chain approach is employed to construct two different initial guesses for the desired transfer. The first leverages only natural dynamical structures while the second includes low-thrust structures. Both orbit chains exploit invariant manifolds.

As expected, the structure of the initial guess biases the solution towards particular characteristics.

Comparison of the optimal low-thrust transfers in Figure 11 reveals the influence of the different initial guesses and the potential benefits offered by including low-thrust dynamical structures. When only natural structures are included in the initial guess, the resulting transfer, appearing in Figure 11(a), includes an extended thrust segment near the initial L_4 SPO to depart this orbit and another brief thrust arc to connect with the stable manifold trajectory of the L_1



(a) Transfer from orbit chain with only natural dynamical structures



(b) Transfer from orbit chain with low-thrust dynamical structures

Fig. 11: Direct transcription is employed to compute mass optimal low-thrust transfers using the orbit chain initial guesses.

Lyapunov orbit. The initial revolution of the L_4 SPO employed in the initial guess remains in place, while the subsequent stacked revolutions are spread over the L_4 region to facilitate the connection with the stable manifold. The time-of-flight for this transfer is approximately 205 days; a transfer with a shorter TOF is likely available if the initial guess is modified to incorporate fewer revolutions of the L_4 SPO.

The transfer constructed with low-thrust dynamical structures, displayed in Figure 11(b), also exhibits loops near L_4 because the low-thrust periodic orbit and manifold trajectory included in the initial guess possess this behavior. The time-of-flight for this transfer is approximately 201 days, consistent with

Init. Guess	TOF [days]	Δm [kg]	ΔV [m/s]
Nat. Only	205.188	2.422	71.331
With LT	200.756	1.518	44.694

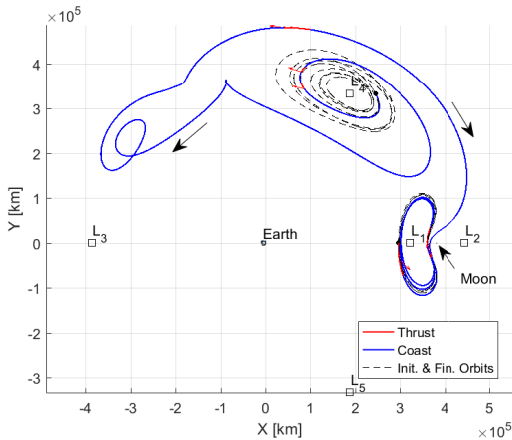
Table 2: Summary of key parameters for the low-thrust transfers computed in the Earth-Moon CR3BP for Application 2.

the initial design. The geometric and time-of-flight differences between the two transfers lead to different propellant usages: 2.422 kg and 1.518 kg (for a 1000 kg spacecraft) for the natural and low-thrust seeded designs, respectively. These differences, summarized in Table 2, may originate within the variability of the solution due to numerical considerations such as node placement. Nonetheless, the transfer generated using low-thrust dynamical structures does require less propellant and ΔV than the alternate case. In addition to this quantitative difference, the inclusion of low-thrust structures also enables an alternative transfer geometry that is well-predicted by the initial design. In this case, the low-thrust manifold geometry is not straightforwardly available from the natural dynamical structures of interest, i.e., the L_1 Lyapunov, its manifolds, and L_4 SPO. The novel geometries, and, in some cases, improved optimal solutions, suggest that there may be benefits to incorporating low-thrust dynamical structures in the transfer design process.

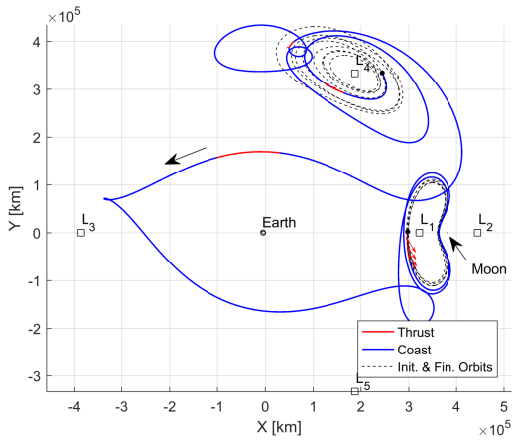
To validate these results both low-thrust transfers are transitioned to an N -body ephemeris model that includes the Earth, Moon, Sun, and Jupiter. The resulting transfers are displayed in Figure 12. Clearly, both transfers retain a similar geometry to that observed in the CR3BP. This result indicates that similar trajectories are available in an ephemeris model and may be leveraged in support of various mission scenarios.

VI. CONCLUDING REMARKS

An orbit chain approach to low-thrust trajectory design enables rapid exploration of the design space afforded by a given dynamical model. Experimentation with the various combinations of dynamical structures that may be incorporated into an orbit chain often reveals different local “basins” of optimal solutions. This investigation demonstrates that dynamical structures generated in the CR3BP-LT can be incorporated into an orbit chain technique in the same manner as natural periodic orbits and manifold trajectories. Through the application of dynamical



(a) Transfer generated with natural dynamical structures.



(b) Transfer generated with low-thrust dynamical structures.

Fig. 12: Direct transcription is employed to compute mass optimal low-thrust transfers in an N -Body ephemeris model using the CR3BP result as an initial guesses.

ical systems theory to the CR3BP-LT, low-thrust enabled dynamical structures with novel geometries and energy profiles may be generated. A new catalog of low-thrust periodic orbits and manifolds offered by the CR3BP-LT permits the assembly of initial guesses with reduced state discontinuities or gaps in energy level, as apparent in the first sample application. This application also illustrates that, despite their unique properties, the inclusion of low-thrust dynamical structures in an orbit chain can sometimes lead to an optimal solution that is nearly identical to one computed with an initial guess comprised of only natural dynamical structures. However, the sec-

ond sample application demonstrates that leveraging low-thrust dynamical structures can offer alternate geometries that may not otherwise be available. This second application leverages a manifold trajectory from an unstable low-thrust periodic orbit to guide the flow away from a naturally stable periodic orbit. Overall, low-thrust dynamical structures offer a new catalog of options that may be leveraged in an orbit chain technique for the computation of optimal low-thrust trajectories. These low-thrust trajectories expand the solution space via different times of flight, propellant consumption, and/or geometric characteristics.

ACKNOWLEDGEMENTS

The authors thank the Purdue University School of Aeronautics and Astronautics for facilities and support, including access to the Rune and Barbara Eliassen Visualization Laboratory. Additionally, many thanks to the Purdue Multi-Body Dynamics Research Group for interesting discussions and ideas. This research is supported by NASA Space Technology Research Fellowships, NASA Grants NNX16AM42H and NNX16AM40H. Some analysis was conducted at the NASA Goddard Space Flight Center. Additionally, portions of this work were completed at the Jet Propulsion Laboratory, California Institute of Technology, under a contract with the National Aeronautics and Space Administration. Government sponsorship acknowledged. © 2018. All rights reserved.

REFERENCES

- [1] M. D. Rayman, P. Varghese, D. H. Lehman, and L. L. Livesay. Results from the Deep Space 1 Technology Validation Mission. *Acta Astronautica*, 47(2-9):475–487, 2000.
- [2] C. Russell and C. Raymond, editors. *The Dawn Mission to Minor Planets 4 Vesta and 1 Ceres*. Springer-Verlag, New York, 1 edition, 2012. ISBN 978-1-4614-4902-7.
- [3] N. Bosanac, A. D. Cox, K. C. Howell, and D. C. Folta. Trajectory design for a cislunar CubeSat leveraging dynamical systems techniques: The Lunar IceCube mission. *Acta Astronautica*, 144: 283–296, 2018.
- [4] D. Y. Oh, S. Collins, D. Goebel, B. Hart, G. Lantoiné, S. Snyder, G. Whiffen, L. Elkins-tanton, P. Lord, Z. Pirkl, and L. Rotlisburger. Development of the Psyche Mission for NASA’s Dis-

- covery Program. In *35th International Electric Propulsion Conference*, Atlanta, Georgia, 2017.
- [5] M. L. Mcguire, L. M. Burke, S. L. McCarty, K. J. Hack, R. J. Whitley, D. C. Davis, and C. Ocampo. Low Thrust Cis-Lunar Transfers Using a 40 kW-Class Solar Electric Propulsion Spacecraft. In *AAS/AIAA Astrodynamics Specialist Conference 2017*, Stevenson, Washington, 2017.
- [6] R. E. Pritchett, K. C. Howell, and D. J. Grebow. Low-Thrust Transfer Design Based on Collocation Techniques: Applications in the Restricted Three-Body Problem. In *AAS/AIAA Astrodynamics Specialist Conference*, Stevenson, Washington, 2017.
- [7] R. E. Pritchett, E. Zimovan, and K. Howell. Impulsive and Low-Thrust Transfer Design Between Stable and Nearly-Stable Periodic Orbits in the Restricted Problem. In *2018 AIAA/AAS Space Flight Mechanics Meeting*, Orlando, Florida, 2018. ISBN 978-1-62410-533-3.
- [8] K. C. Howell, B. T. Barden, and M. W. Lo. Application of Dynamical Systems Theory to Trajectory Design for a Libration Point Mission. *The Journal of the Astronautical Sciences*, 45(2):161–178, 1997.
- [9] W. S. Koon, M. W. Lo, J. E. Marsden, and S. D. Ross. Heteroclinic connections between periodic orbits and resonance transitions in celestial mechanics. *Chaos: An Interdisciplinary Journal of Nonlinear Science*, 10(2):427–469, 2000.
- [10] G. Gómez, W. S. Koon, M. W. Lo, J. E. Marsden, J. J. Masdemont, and S. D. Ross. Connecting orbits and invariant manifolds in the spatial restricted three-body problem. *Nonlinearity*, 17(5):1571–1606, 2004.
- [11] S. Ross and M. Lo. The lunar L1 gateway-portal to the stars and beyond. In *AIAA Space 2001 Conference and Exposition*, pages 47–68, Albuquerque, New Mexico, 2001.
- [12] M. Vaquero and K. C. Howell. Leveraging Resonant-Orbit Manifolds to Design Transfers Between Libration-Point Orbits. *Journal of Guidance, Control, and Dynamics*, 37(4):1143–1157, 2014.
- [13] A. F. Haapala and K. C. Howell. A Framework for Constructing Transfers Linking Periodic Libration Point Orbits in the Spatial Circular Restricted Three-Body Problem. *International Journal of Bifurcation and Chaos*, 26(05), 2016.
- [14] J. S. Parker, K. E. Davis, and G. H. Born. Chaining periodic three-body orbits in the Earth-Moon system. *Acta Astronautica*, 67(5-6):623–638, 2010.
- [15] M. W. Lo and J. S. Parker. Chaining Simple Periodic Three Body Orbits. In *AAS/AIAA Astrodynamics Specialist Conference*, Lake Tahoe, California, 2005.
- [16] R. L. Restrepo and R. P. Russell. A Database of Planar Axi-Symmetric Periodic Orbits for the Solar System. Stevenson, Washington, 2017.
- [17] R. L. Restrepo and R. P. Russell. Patched Periodic Orbits: A Systematic Strategy for Low Energy Transfer Design. Stevenson, Washington, 2017.
- [18] A. Das-Stuart, K. C. Howell, and D. C. Folta. A rapid trajectory design strategy for complex environments leveraging attainable regions and low-thrust capabilities. In *68th International Astronautical Congress*, Adelaide, Australia, September 2017.
- [19] M. Canon, C. Cullum, and E. Polak. *Theory of Optimal Control and Mathematical Programming*. McGraw-Hill, New York, 1970.
- [20] D. J. Grebow and T. A. Pavlak. MColl: Monte Collocation Trajectory Design Tool. In *AAS/AIAA Astrodynamics Specialist Conference*, Stevenson, Washington, 2017.
- [21] J. T. Betts. Survey of Numerical Methods for Trajectory Optimization. *Journal of Guidance, Control, and Dynamics*, 21(2):193–207, 1997.
- [22] F. Topputo and C. Zhang. Survey of Direct Transcription for Low-Thrust Space Trajectory Optimization with Applications. *Abstract and Applied Analysis*, 2014, 2014.
- [23] B. A. Conway. A Survey of Methods Available for the Numerical Optimization of Continuous Dynamic Systems. *Journal of Optimization Theory and Applications*, 152(2):271–306, 2012.
- [24] M. T. Ozimek, D. J. Grebow, and K. C. Howell. A Collocation Approach for Computing Solar Sail Lunar Pole-Sitter Orbits. *Open Aerospace Engineering Journal*, 3:65–75, 2010.
- [25] M. T. Ozimek. *Low-Thrust Trajectory Design and Optimization of Lunar South Pole Coverage Missions*. Ph.D. dissertation, Purdue University, 2010.
- [26] J. F. C. Herman. *Improved Collocation Methods to Optimize Low-Thrust, Low-Energy Transfers in the Earth-Moon System* by. Ph.D. dissertation, University of Colorado, Boulder, Colorado, 2015.

- [27] N. L. Parrish, J. S. Parker, S. P. Hughes, and J. Heiligers. Low-Thrust Transfers From Distant Retrograde Orbits To L2 Halo Orbits in the Earth-Moon System. In *International Conference on Astrodynamics Tools and Techniques*, Darmstadt, Germany, 2016.
- [28] A. Petropoulos and J. Sims. A review of some exact solutions to the planar equations of motion of a thrusting spacecraft. In *2nd International Symposium on Low Thrust Trajectories*, Toulouse, France, June 2002.
- [29] S. Hernandez. *Low-Thrust Trajectory Design Techniques with a Focus on Maintaining Constant Energy*. Ph.D. dissertation, University of Texas at Austin, Austin, Texas, August 2014.
- [30] C. R. McInnes, A. J. C. McDonald, J. F. L. Simmons, and E. W. MacDonald. Solar sail parking in restricted three-body systems. *Journal of Guidance, Control, and Dynamics*, 17(2), March-April 1994.
- [31] A. Farrés and À. Jorba. Solar sail surfing along families of equilibrium points. *Acta Astronautica*, 63:249–257, July 2008.
- [32] A. Farrés and À. Jorba. Periodic and quasi-periodic motions of a solar sail close to SL_1 in the earth-sun system. *Celestial Mechanics and Dynamical Astronomy*, 107(1-2):233–253, June 2010.
- [33] A. Farrés. Transfer orbits to L4 with a solar sail in the earth-sun system. *Acta Astronautica*, 137: 78–90, 2017.
- [34] A. D. Cox, K. C. Howell, and D. Folta. Dynamical structures in a combined low-thrust multi-body environment. In *AAS/AIAA Astrodynamics Specialist Conference*, Columbia River Gorge, Stevenson, Washington, August 2017.
- [35] A. D. Cox, K. C. Howell, and D. Folta. Trajectory design leveraging low-thrust, multi-body equilibria and their manifolds. In *AAS/AIAA Astrodynamics Specialist Conference*, Snowbird, Utah, August 2018.
- [36] V. Szebehely. *Theory of Orbits: The Restricted Problem of Three Bodies*. Academic Press, 1967.
- [37] C. H. Acton. Ancillary data services of nasas navigation and ancillary information facility. *Planetary and Space Science*, 44(1):65–70, 1996.
- [38] D. A. D. Tos and F. Topputo. Trajectory refinement of three-body orbits in the real solar system model. *Advances in Space Research*, 59(8):2117–2132, 2017.
- [39] W. S. Koon, M. W. Lo., J. E. Marsden, and S. D. Ross. *Dynamical Systems, the Three-Body Problem and Space Mission Design*. Springer, New York, 2011.
- [40] M. W. Lo, B. G. Williams, W. E. Bollman, D. Han, Y. Hahn, J. L. Bell, E. A. Hirst, R. A. Corwin, P. E. Hong, K. C. Howell, B. T. Barnden, and R. S. Wilson. Genesis mission design. *The Journal of Astronautical Sciences*, 49(1):169–184, 2001.